Biomaterials and Biosystems 14 (2024) 100095

Contents lists available at ScienceDirect

Biomaterials and Biosystems

journal homepage: www.elsevier.com/locate/bbiosy

Bifunctional mesoporous glasses for bone tissue engineering: Biological effects of doping with cerium and polyphenols in 2D and 3D in vitro models

Ksenia Menshikh [a,1], Ajay Kumar Reddy [a,1], Andrea Cochis [a], Francesca Fraulini [b], Alfonso Zambon [b], Gigliola Lusvardi [b,*], Lia Rimondini [a,*]

[a] Center for Translational Research on Autoimmune and Allergic Disease—CAAD, Department of Health Sciences, Università del Piemonte Orientale, Novara 28100, Italy
[b] Department of Chemical and Geological Sciences, University of Modena and Reggio Emilia, Modena 41125, Italy

ARTICLE INFO

Keywords:
Mesoporous bioactive glasses
Cerium
Polyphenols
Cytocompatibility
3D *in vitro* models

ABSTRACT

This study evaluates the cytocompatibility of cerium-doped mesoporous bioactive glasses (Ce-MBGs) loaded with polyphenols (Ce-MBGs-Poly) for possible application in bone tissue engineering after tumour resection. We tested MBGs powders and pellets on 2D and 3D *in vitro* models using human bone marrow-derived mesenchymal stem cells (hMSCs), osteosarcoma cells (U2OS), and endothelial cells (EA.hy926). Promisingly, at a low concentration in culture medium, Poly-loaded MBGs powders containing 1.2 mol% of cerium inhibited U2OS metabolic activity, preserved hMSCs viability, and had no adverse effects on EA.hy926 migration. Moreover, the study discussed the possible interaction between cerium and Poly, influencing anti-cancer effects. In summary, this research provides insights into the complex interactions between Ce-MBGs, Poly, and various cell types in distinct 2D and 3D *in vitro* models, highlighting the potential of loaded Ce-MBGs for post-resection bone tissue engineering with a balance between pro-regenerative and anti-tumorigenic activities.

Abbreviations

BGs	bioactive glasses
MBGs	mesoporous bioactive glasses
Ce-MBGs	cerium-doped mesoporous bioactive glasses
Poly	polyphenols

1. Introduction

Biomaterials, and specifically bioactive glasses (BGs), have been widely studied and used for the treatment of bone defects, as they are able to bind to the bone and stimulate osteogenesis through the release of biologically active ions (bioactivity) [1–3]. The implant of a biomaterial often creates an inflammatory state with the production of reactive oxygen species (ROS) that can require lengthy drug treatments. In recent years, research in the field has focused on the development of biomaterials with antioxidant properties that can convert ROS into non-hazardous species and reduce post-implantation complications [4–7]. To this end, one strategy employed is the doping of BGs with therapeutic inorganic ions (TIIs), which can confer antioxidant and/or osteogenic, angiogenic, cementogenic and antibacterial properties on the BGs [8–10]. Among TIIs, cerium exhibits significant antioxidant and anti-inflammatory activities for its ability to quench ROS and regulate their level within the microenvironment and is thus of particular interest. Cerium-based compounds have long shown relevant pharmacological properties and have been used, for example, as antiemetics, bacteriostats and anticancer agents [11–19].

Another well-established strategy to confer desirable biological properties on BGs is their loading with organic compounds able to elicit specific cellular responses onto the target tissue. These compounds include drugs and biomolecules and can add antioxidant properties, but also antitumour, antibacterial, anti-inflammatory, vasoprotective and bone-promoting effects to the loaded biomaterial [1,20–31]. Recently, we evaluated the effect of the loading of biomolecules (such as gallic acid, anthocyanins and polyphenols) on the antioxidant properties of Ce-doped BGs (specifically, mesoporous bioactive glasses, Ce-MBGs). We found that doping with cerium does not affect the bioactivity of the BGs while having a positive effect on their biocompatibility and giving the materials the ability to dismutate hydrogen peroxide, one of the main ROS species [16]. The loading of Ce-MBGs with polyphenols

* Corresponding authors.
E-mail addresses: gigliola.lusvardi@unimore.it (G. Lusvardi), lia.rimondini@med.uniupo.it (L. Rimondini).
[1] Co-shared First Authors – equal input from both authors in the manuscript.

https://doi.org/10.1016/j.bbiosy.2024.100095
Received 27 March 2024; Received in revised form 9 May 2024; Accepted 24 May 2024
Available online 31 May 2024

(Ce-MBGs-Poly) removes a second important ROS species, the superoxide anion, presumably by radical scavenging. Doping with cerium and loading with Poly thus add complementary antioxidant properties to MBGs, while maintaining their bioactivity.

In bone healing, osteogenesis and angiogenesis processes are closely connected. Newly formed vessels deliver not only necessary nutrients but also differentiation factors. Thus, it is of particular importance that the biomaterials designed for bone tissue engineering promote – or, at least, do not interfere in – angiogenesis [32]. Extracts of cerium-containing bioactive glasses were shown to promote proliferation, migration and lymphatic vascular network formation in an *in vitro* model set up with the use of lymphatic endothelial cells [33].

Bone regeneration is a coordinated action of multiple cell types, such as mesenchymal stem cells, osteoblasts, chondrocytes, and immune and endothelial cells, which is why it is important to test material in various *in vitro* models [34]. Additionally, for a multifunctional material aiming not only at assisting bone regeneration but also at suppressing cancer cell activity – which may be the case on the site of bone cancer resection – the activity towards cancer cells should also be taken into account [35]. Other factors, *e.g.,* form, surface area and particle size of the material are to be considered in the design of the experiment to avoid interferences such as excessive absorption of nutrients from culture medium or blocking gas exchange by the material [36–38]. Nowadays, there is no universal testing method available that could be sufficient and applicable for a comprehensive biological evaluation of materials for bone repair. For these reasons, in the design of our study, we exploited different cell lines, as well as 2D and 3D *in vitro* models.

This study aims to evaluate the *in vitro* performance of Ce-MBGs and Ce-MBGs-Poly towards cell lines representing the bone microenvironment. First, to assess the cytocompatibility of the materials, we tested them in conventional 2D-monolayer *in vitro* models simulating "physiological" and "pathological" conditions – with human bone marrow-derived mesenchymal stem cells and human osteosarcoma cells, respectively. In the following steps, the cytocompatibility was evaluated in a 3D spheroid-based set-up using the same cell lines. Next, considering angiogenesis as a key factor in bone regeneration, we analysed the influence of Ce-MBGs on endothelial cell migration. Finally, considering the potential application of these materials, pellets of Ce-MBGs were produced and tested *in vitro* towards all three above-mentioned cell lines.

2. Materials and methods

2.1. MBGs production

Ce-MBGs were synthesized using the modified sol-gel evaporation-induced self-assembly process (EISA) method as previously described [12,39]; they were then ground to obtain powders in the range of 50–150 μm. The nominal composition is reported in Table S1 and was verified by X-ray fluorescence spectroscopy (XRF) as previously described [39]. The same powders were pressed to obtain pellets of 12 mm in diameter and 1 mm in height.

Poly loading was performed as previously reported [16] using a mixture of Poly extracted from chestnut flour. 1.0 mg/mL of loading solution was prepared by dissolving Poly mixture in double-distilled water for 2 hrs under magnetic stirring. Loading was performed by soaking 0.1 g of each MBGs for 3 hrs at 37 °C in 5 mL of loading solution. All samples were covered with aluminium foil to avoid exposure to light.

2.2. MBGs characterization

2.2.1. UV–Vis analyses - Folin&Ciocalteau (F&C) method – Gallic Acid Equivalents (GAE) determination

A modified Folin&Ciocalteau (F&C) method was utilised to quantify the amount of Poly loaded onto the MBGs directly on the solid mixture [16]. The results are reported as a percentage of Gallic Acid Equivalents (GAE), the most common spectrophotometric parameter for the estimation of antioxidant properties. 0.1g of each grafted MBG was mixed with 8 mL of double distilled water, 0.5 mL of F&C reagent (Sigma-Aldrich), and 1.5 mL of 20 % (p/V) Na_2CO_3 (Sigma-Aldrich) solution. After 2 hrs, UV–Vis measurements were carried out on the resulting solution by means of UV–Vis Spectrophotometer (JASCO V-570). A calibration curve was prepared with eight solutions at defined GA concentrations (0.0015, 0.0030, 0.0060, 0.0090, 0.0150, 0.0300, 0.0600 and 0.3000 mg/mL). The results are reported as GAE% in weight.

2.2.2. Elemental analysis

Elemental analysis was carried out with a FLASH 2000 Thermo Fisher analyser in order to quantify the Poly amount in the loaded MBGs by the measurement of carbon content (%C). These results are then compared with those obtained with the F&C method; it must be noted that this comparison holds only qualitative values for Poly which are complex mixtures of several biomolecules of variable molecular weight.

2.2.3. Specific surface area (SSA) determination

Specific surface area (SSA) was evaluated before and after loading in order to assess possible textural changes arising from this process. SSA was determined by nitrogen adsorption porosimetry using a Micromeritics Chemisorb 2750 and the Brunauer-Emmett-Teller (BET) method.

2.3. Cell lines and culturing conditions

Human bone marrow-derived stem cells (hMSCs Y201) were kindly provided by Prof. P. Genever, University of York. They were isolated from bone marrow and immortalized through the hTERT lentiviral vector as described previously [40]. Cells were cultivated in low-glucose Dulbecco's Modified Eagle Medium (DMEM, Sigma-Aldrich, USA) supplemented with 15 % fetal bovine serum (FBS, Sigma-Aldrich, USA) and 1 % penicillin-streptomycin (PS, Invitrogen, USA). Human osteosarcoma cells (U2OS, HTB96, American Type Culture Collection, Manassas, VA, USA) and human endothelial umbilical vein cells (EA.hy926, American Type Culture Collection, Manassas, VA, USA, CRL-2922) were cultivated in high-glucose DMEM (Sigma-Aldrich, USA) supplemented with 10 % FBS and 1 % PS. All cell lines were cultivated at 37 °C in the humidified atmosphere containing 5 % CO_2. Before experiments, cells were cultivated until 80–90 % confluence, detached by trypsin-EDTA solution (Sigma-Aldrich, USA), harvested, and used for experiments.

2.4. MBGs powders preparation for in vitro assays

MBGs powders were weighed and sterilized by heating at 160 °C for 2 hrs or, in the case of Poly-loaded powders, disinfected by UV exposure for 20 mins [19,33]. Prior to each experiment, MBGs powders were quickly washed with phosphate-buffered saline (PBS, Sigma-Aldrich, USA). All MBGs (Table S1) were tested at concentrations of 1 and 5 mg/mL.

2.5. 2D cytocompatibility assay

For the monolayer-based cytocompatibility assay, hMSCs and U2OS cells were seeded in a 24-well plate in a defined concentration (1×10^4 cells/well) and allowed to adhere and spread overnight. After this, the culture medium in the wells was substituted with MBGs powders suspension in the culture medium at concentrations 1 and 5 mg/mL. Fresh culture medium was added to the control, and cells were cultivated for 3 days.

On the 1st and 3rd days, the metabolic activity of the cells was evaluated by the fluorescent Alamar blue assay (alamarBlue™, Life Technologies, USA) following the manufacturer's instructions. Briefly, supernatants were removed from each well and replaced with Alamar blue solution in fresh culture medium. Plates were incubated in the dark

for 4 hrs, and then 100 μL were transferred into a black opaque 96-well plate and read with a spectrophotometer (Spark®, Tecan Trading AG, CH) using the following set-up: fluorescence excitation wavelength at 570 nm, emission reading at 590 nm. Results were presented in relative fluorescent units (RFU).

After the metabolic activity assay on the last day of the experiment, we furthermore visualized the hMSCs and U2OS cell morphology by staining the cytoskeleton. For this, cells were washed with PBS and fixed with 4 % paraformaldehyde (reagent grade, crystalline, Sigma-Aldrich, USA) solution at room temperature for 20 mins. Cells were washed with PBS again to eluate the fixative reagent and permeabilized for 10 mins with 0.5 % Triton in PBS (Triton™ X-100, Sigma-Aldrich, USA) at RT. Furthermore, Alexa Fluor™ 488 Phalloidin (Life Technologies, USA) and 4,6-diamidino-2-phenylindole (DAPI, Sigma-Aldrich, USA) in PBS were added and incubated for 40 mins at RT. Images were obtained with the EVOS Floid Microscope Imaging System (Invitrogen, USA).

2.6. 3D cytocompatibility assay

For the spheroid-based cytocompatibility assay, firstly, wells of a 48-well plate were coated with 1.5 % agarose solution in sterile conditions and let solidify and disinfect at RT under UV exposure for 2 hrs. Then, hMSCs and U2OS cells were seeded in the amount of 5×10^4 cells per well of the agarose-coated plate. Cells were incubated in standard conditions with the medium being changed every 2 or 3 days. After the 7 days of complete self-aggregation of spheroids confirmed by light microscopy, the culture medium in the wells was substituted with MBGs powder suspension in the culture medium at concentrations of 1 and 5 mg/mL. Fresh culture medium was added to the control, and spheroids were cultivated for 7 days. By introducing the 7th-day time point we aim at detecting possible effects which might not be present at the earlier time points due to the features of the spheroids – their permeability and the presence of cells which are not directly exposed to the tested materials.

Metabolic activity assay was performed on the 1st, 3rd and 7th days as described above. Additionally, the cell viability was further confirmed by evaluating them with the fluorescent live/dead assay (LIVE/DEAD, Invitrogen, L3224, Thermo Fisher, USA) following the manufacturer's instructions. Briefly, 2 μM Calcein AM and 4 μM Ethidium Homodimer-1 (EthD-1) solutions in fresh culture medium were added to spheroid-containing wells and then incubated in the dark for 45 min. After incubation, spheroids were visualized with Leica THUNDER Imager 3D Live Cell (Leica Microsystems, USA).

2.7. MBGs extracts angiogenic potential assay

To estimate the potential influence of MBGs on angiogenesis, an endothelial cell spheroid migration assay was set up. For this, spheroids of endothelial EA.hy926 cells were prepared as described above. After spheroid maturation, spheroids were transferred to a new 24 multi-well plate and let adhere overnight. Ce-MBGs and Ce-MBGs-Poly weighed and sterilized powders were transferred into sterile 15-mL tubes and resuspended in a complete medium (up to concentrations of 1 and 5 mg/mL). Tubes were incubated at 37 °C, 5 % CO_2 in the humidified atmosphere, and extracts were obtained and added to the spheroids. Spheroid migration was assessed after 0, 24, 48 and 72 hrs of incubation with extracts. At each time point, phase-contrast light microscopy images of spheroids were collected, and results were analysed in the ImageJ software with the use of a free toolset for cell invasion analysis (Analyse Spheroid Cell Invasion In 3D Matrix, RRID: SCR_021204 [41]).

2.8. MBGs pellets cytocompatibility assay

Biological characterization of 12-mm MBGs pellets (Table S2) was performed on hMSCs, U2OS and EA.hy926 cells. Prior to incubation in direct contact with cells, the specimens were disinfected by UV exposure for 1 h and placed in a 24-well plate.

Cells were seeded dropwise directly onto the specimens' surface at a defined concentration (1.5×10^4 cells/specimen), allowed to adhere for 2 hrs, and then 1 mL of a relevant culture medium was added to the well. Cell-seeded pellets were incubated for 4 days. On the 1st, 3rd and 4th days, the metabolic activity of the cells in direct contact with specimens was evaluated by the fluorimetric Alamar blue assay, as described before.

2.9. Statistical analysis

Each group of samples was represented by three replicates. Results are shown as mean value ± standard deviation. Comparison between groups within experimental time points was performed in Prism (v8, GraphPad Software, USA) using two-way ANOVA with Dunnett's correction. Before that, Shapiro–Wilk's test for normal distribution and ROUT (Robust regression and Outlier removal) method for outliers' identification were performed. For each comparison, the difference was determined as significant for $p < 0.05$.

3. Results

3.1. MBGs characterization

Loading values on the Ce-MBGs-Poly powders were confirmed to be around 1 %, by elemental analysis and F&C method, in agreement with our previous results [16].

SSA of Ce-MBGs before and after Poly loading are reported in Fig. S1. All unloaded Ce-MBGs present SSA values around 300 m^2/g regardless of their cerium content, as previously observed; these values are consistent with the mesoporous nature of the glasses [12,16,42]. Loading with Poly results in a significant reduction of SSA to around 100 m^2/g regardless of the cerium amounts. SSA values were optimised compared to previous works using a thermoshaker in order to achieve a more homogeneous loading.

3.2. MBGs powders cytocompatibility assay: 2D

In-vitro evaluation of MBGs powders' cytocompatibility was done towards hMSCs, which were selected as representatives of the self-healing process during bone regeneration. The other cell line of choice for this assay was the osteoblast-like osteosarcoma U2OS cell line, frequently used both as a representative of the osteoblast compartment of the bone microenvironment and as a model to test anticancer activity. First, we incubated MBGs powders with cells in a standard 2D monolayer to evaluate the direct influence of the material on cell metabolic activity.

The complete results of the cytocompatibility assay toward hMSCs are presented in Fig. S2, and the results of the terminal time point are in Fig. 1 (a). After 1 day of direct contact, there is no significant difference in hMSCs metabolic activity observed between control and Ce-MBGs at 1 and 5 mg/mL and Ce-MBGs-Poly, at 1 mg/mL (Fig. S2(a)). Ce-MBGs-Poly at 5 mg/mL negatively influence the cell metabolic activity at the highest cerium amounts (3.6 and 5.3 mol %). On the 2nd day of cultivation, the relative metabolic activity of cells drops in the majority of groups of Ce-MBGs and Ce-MBGs-Poly at 1 mg/mL except those with the highest cerium amount, and in all groups at 5 mg/mL except MBG-Poly; however, this group is still significantly lower than the control in terms of raw RFU values. On the 3rd day, it remains low for MBGs without cerium (1 and 5 mg/mL) and MBG1.2 at 1 mg/mL (Fig. 1 (a)). The same trend is observed for Ce-MBGs-Poly on the 3rd day at 1 mg/mL; at 5 mg/mL, on the contrary, the lowest metabolic activity is observed for the group with the highest amount of cerium (MBG5.3 Poly). In summary, both Ce-MBGs and Ce-MBGs-Poly are generally well tolerated. Without Poly for both concentrations and with Poly at 1 mg/mL, the lowest hMSCs cell metabolic activity is correlated with the lowest cerium

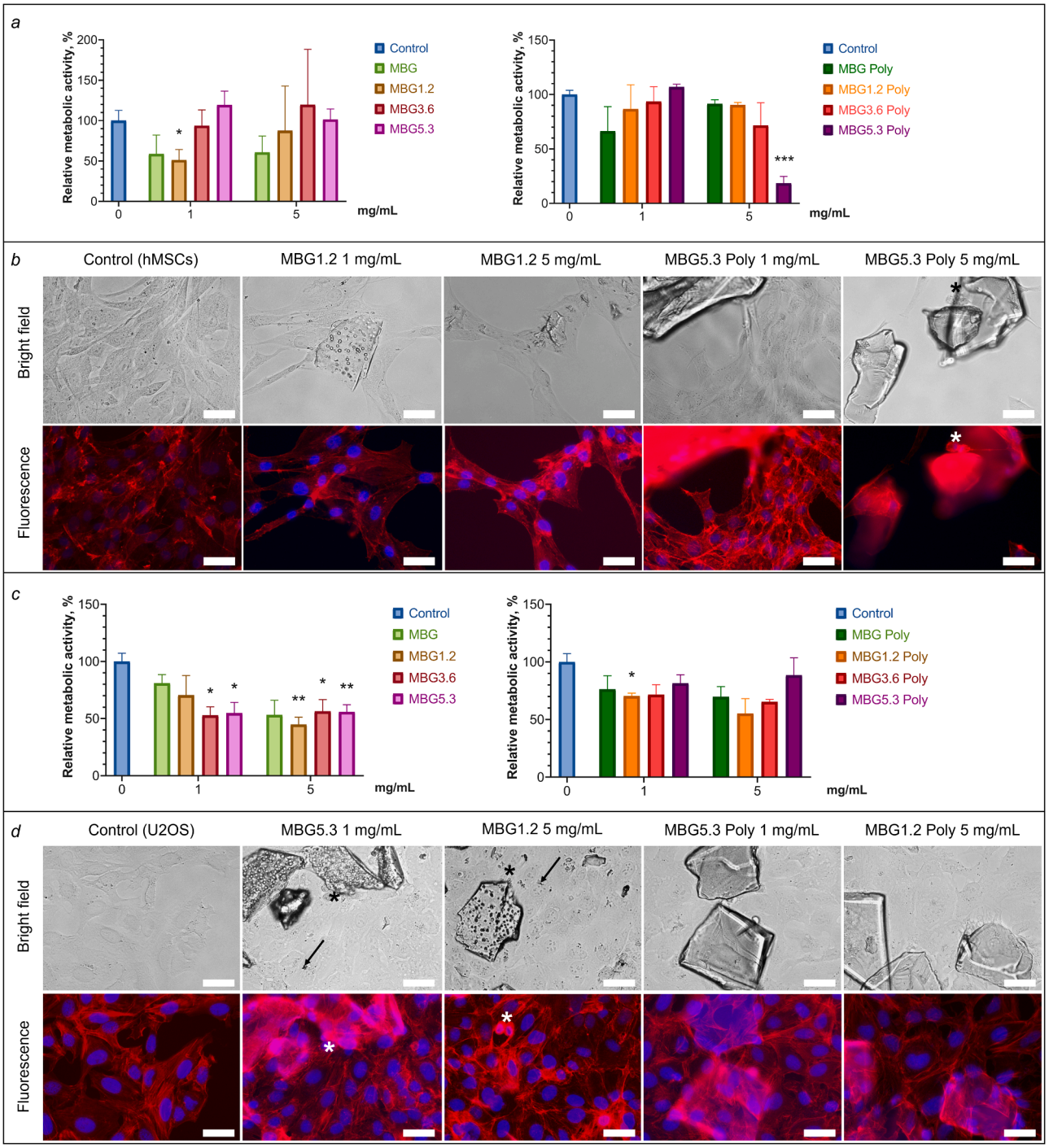

Fig. 1. Metabolic activity of hMSCs (a) and U2OS (c) cells cultivated for 72 hrs in direct contact with Ce-MBGs and Ce-MBGs-Poly powders (1 and 5 mg/mL). 'Control' represents cells cultivated in the medium without powders addition. The values are presented as mean ± SD of relative cell viability. Statistical analysis was performed on relative fluorescent units (RFU) of three biological replicates, * - significant differences compared to control, $p < 0.05$; ** - $p < 0.01$; *** - $p < 0.001$. Panels b and d: cell morphology evaluation after 72 hrs of cultivation in direct contact with Ce-MBGs and Ce-MBGs-Poly powders. Actin cytoskeleton is stained red (Phalloidin) and nuclei are stained blue (DAPI). Asterisks indicate cells with altered morphology in contact with powders. Arrows indicate powders attached to the U2OS cells in the samples of Ce-MBGs, which is not the case in Ce-MBGs-Poly (clearer area). Scale bar 25 μm.

amount; in contrast, the highest cerium amount (5.3 mol %) in the Ce-MBGs-Poly at 5 mg/mL negatively affects cell viability.

The results of the metabolic activity assay on U2OS differ markedly from those of hMSCs. For instance, on the 1st day relative cell viability is above the 70 % threshold and there are no significant differences between the control and experimental groups except for the group Ce-MBG1.2 at 5 mg/mL (Fig. S2(b)). On the 2nd day, there is a decrease in metabolic activity in most of the experimental groups in comparison to the control. The 3rd day of incubation also resulted in an overall decrease in metabolic activity, but much less marked for the Ce-MBGs-Poly group (Fig. 1 (c)). In summary, Poly loading seems to compensate for the detrimental effect of cerium doping on the viability of U2OS cells.

In addition to the metabolic activity assay, cells cultivated in direct contact with the Ce-MBGs powders were visualized using fluorescence microscopy to detect possible cell morphology alterations and particle

internalization. The selected images are presented in Fig. 1 (b) and (d), additional images can be found in Fig. S3. No changes in hMSCs morphology were visible: cells had elongated morphology and were well spread in the presence of powders (Fig. 1 (b)). Moreover, Ce-MBGs powders were strongly attached to cells at all concentrations, which could also explain a slightly lower confluency of these samples: due to aggregation with particles, cells might have been rinsed off during the staining procedure. As for Ce-MBGs-Poly, the morphology of hMSCs was also found normal; in comparison to the Ce-MBGs groups, larger particles were attached to the cells. Very low confluency was observed in the group of MBG5.3 Poly 5 mg/mL with still some particles strongly attached to the remaining cells, in line with the metabolic activity results.

Conversely, U2OS cell morphology was frequently found altered in the groups of Ce-MBGs – in particular, for the cells attached to powders. In contrast, there was no alteration in morphology observed in the groups of Ce-MBGs-Poly even in the cells attached to powders (Fig. 1 (d)).

3.3. MBGs powders cytocompatibility assay: 3D

After performing the cytotoxicity assay in a 2D monolayer, we further evaluated the MBGs powders in a 3D spheroid-based model in a prolonged direct contact experiment. In Fig. 2, we present the results of the terminal point (1 week) of the metabolic activity assay; the other time points can be found in Fig. S4.

On day 1, hMSCs cell viability for Ce-MBGs at both 1 and 5 mg/mL is slightly higher than control for the groups with higher cerium content (MBG3.6 and MBG5.3), while being significantly higher than control on day 3 for all cerium-doped groups (Fig. S4(a)). For Ce-MBGs-Poly, cell viability is significantly higher than control for all groups on the 1st day both at 1 and 5 mg/mL, and comparable to control on day 3. After 1 week, Ce-MBGs are generally in line with the control, and Ce-MBGs-Poly are generally slightly lower, except for the MBG5.3 Poly group at 5 mg/mL (Fig. 2 (a)). Interestingly then, both doping with cerium and Poly loading seem to boost spheroids growth at early time points, but this effect wanes at longer cultivation times.

In the case of U2OS spheroids, after 1 day of incubation with Ce-MBGs powders in both concentrations, the spheroids demonstrate significantly lower metabolic activity compared to the control, however, with some groups being still higher than the cell viability threshold (Fig. S4(b)). On day 3, Ce-MBGs are in line with controls for both concentrations, while at the 7-day point cell viability for the Ce-MBGs is somewhat lower than control, with the no-cerium MBG group being significantly lower for both concentrations (Fig. 2 (c)). Remarkably, Ce-MBGs-Poly show a different behavior, having a higher viability (albeit not significantly so) on the 1st day for the MBG3.6 Poly and MBG5.3 Poly at both concentrations and generally viabilities comparable to control at later time points for all groups and concentrations. In summary, at early time points, cerium doping seems to decrease U2OS spheroid growth while further functionalization with Poly seems to promote it, and at later time points, the presence of MBGs does not seem to affect spheroid growth for U2OS.

In addition to the metabolic activity assay, spheroids cultivated in direct contact with the MBGs powders were visualized using light microscopy and fluorescent microscopy with Live/Dead staining to assess the possible change in morphology of the cell spheroids. Fig. 2 (b) illustrates the control hMSCs spheroids and one of the spheroids that demonstrated the lowest viability rates. Interestingly, even though the spheroids were disaggregated throughout the experiment by the 2-week time point, cells of the disaggregated spheroid were attached to MBGs powders lining their surface.

As for the visual observation of U2OS spheroids, spheroids in all groups including control tend to disaggregate with time, while when cultivated with MBGs powders, cells aggregate with the adjacent powders, therefore forming stable units. Staining live U2OS cells with Calcein AM and visualization via fluorescent microscopy confirmed the cells' aggregation to MBGs powders and demonstrated their viability (Fig. 2 (d)). The cells were seen to attach to MBGs powders lining their surface. Bright-field images of hMSCs and U2OS spheroids at the other time points can be observed in Fig. S5.

3.4. MBGs extracts angiogenic potential assay

After performing the 2D-monolayer and 3D-spheroid cytocompatibility of MBGs powders, we further investigated the potential influence of the material on angiogenesis by setting up a spheroid migration assay. Fig. 3 (a) illustrates the principle of the assay on the example of the control and MBG5.3 Poly 5 mg/mL groups; other groups are presented in Supplementary (Figs. S6–S9).

Quantitative analysis does not provide any evidence of any significant influence on endothelial cell migration in any of the experimental groups throughout the first 24 hrs. Migration was also not altered at 48 hrs in the case of Ce-MBGs, whereas it was inhibited by the extract of MBG3.6 Poly at the concentration of 1 mg/mL and MBG Poly, MBG3.6 Poly, and MBG5.3 Poly of 5 mg/mL. By the 3rd day, in most of the spheroids monitored, there was a complete spread of cells within the area of observation. Inhibition of migration was only observed in two samples of 5 mg/mL – MBG3.6 and MBG5.3 Poly (Fig. 3 (b)). Thus, extracts of the lowest (1 mg/mL) MBGs powders concentrations had no inhibition effect on the migration of endothelial EA.hy926 cells from spheroid to monolayer. High concentrations of Poly-loaded powders inhibited the migration at 48 hrs. However, by the end of the experiment, only marginal inhibition was observed in some groups of Ce-MBGs and Ce-MBGs-Poly at 5 mg/mL (MBG3.6 and MBG5.3 Poly).

***

The results of the 2D-based and 3D-based MBGs cytocompatibility assays performed on hMSCs, U2OS, and EA.hy926 are summarized in Fig. 4. In order to avoid overload with data, only the most significant time points are reported (3 days in the case of monolayer-based cytotoxicity, 7 days in the case of spheroid-based cytotoxicity assays, and all affected time points in the case of endothelial cell migration assay).

3.5. MBGs pellets cytocompatibility assay

The aim of the Ce-MBGs and Ce-MBGs-Poly powders is to promote bone repair by direct placement into the bone tumor resection site. So, the powders were compressed into pellets, and their cytocompatibility was assessed *in vitro* towards hMSCs and EA.hy926 in direct contact. Moreover, we studied the possible toxic effect of cerium and/or Poly released from the MBGs pellets on U2OS. Due to the irrelevance of the comparison of cells seeded on polystyrene to cells seeded on the surface of the pellets, the results were normalized and are reported as relative cell viability.

As shown in Fig. 5 (a), left panel, for the viability of hMSCs after 1, 3, and 4 days of cultivation on the pellets, no difference was noticed between MBG and MBG1.2, whereas in MBG3.6 and MBG5.3 the cell viability was almost two times lower. This trend was observed at all time points, however, neither of the groups demonstrated any remarkable changes in relative cell viability between time points. As shown in Fig. 5 (a), right panel, Ce-MBGs-Poly pellets appeared to be more cytocompatible in comparison with the MBG Poly without cerium; the loading with Poly concomitant with cerium doping thus preserves cell metabolic activity.

In the case of direct contact with endothelial cells, both Ce-MBGs and Ce-MBGs-Poly did not show any cytotoxic effect on EA.hy926, and the cells showed an increase in metabolic activity, especially evident from 3 days onwards when cultured with all Ce-MBGs and with MBG5.3 Poly pellets in comparison to MBG and MBG Poly, respectively (Fig. 5 (b)).

The pellets' compatibility was tested in direct contact with U2OS to assess the potential antitumor activity of cerium and Poly. Generally, in function of time, all tested groups resulted in a gradual decrease in cell

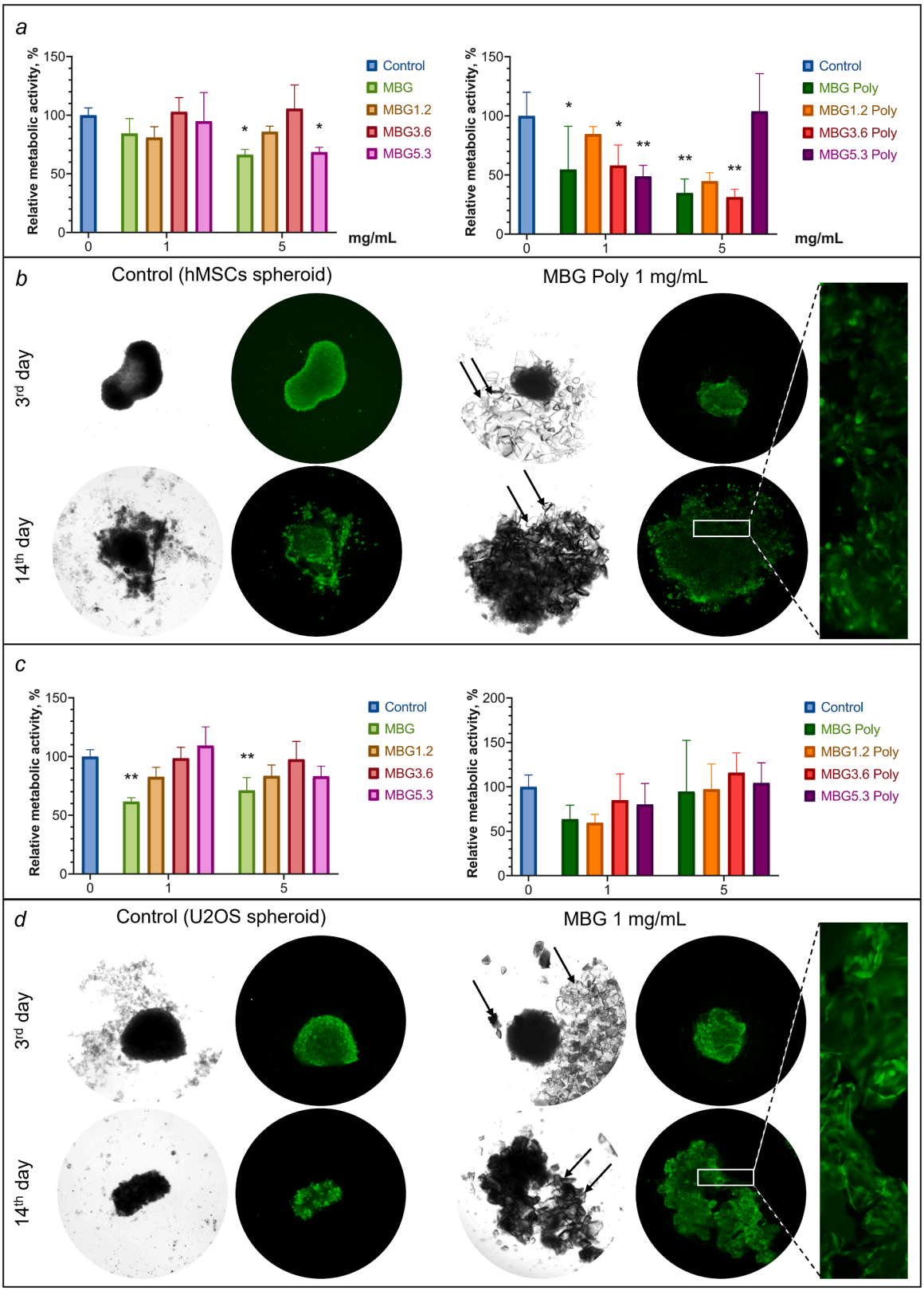

Fig. 2. Metabolic activity of hMSCs (*a*) and U2OS (*c*) cell spheroids cultivated for 1 week in direct contact with Ce-MBGs and Ce-MBGs-Poly powders (1 and 5 mg/mL). 'Control' represents cells cultivated in the medium without powder addition. The values are presented as mean ± SD of relative metabolic activity. Statistical analysis was performed on relative fluorescent units (RFU) of three biological replicates, * - significant differences compared to control, $p < 0.05$; ** - $p < 0.01$; *** - $p < 0.001$. Panels *b* and *d*: bright-field and fluorescent microscopy images of cell spheroids formed from 5×10^4 cells cultivated in standard conditions (Control) and MBGs powders for 3 days and 2 weeks. Live cells stained green (Calcein AM). The channel of EthD-1 staining is not presented due to the absence of dead cells in the area of observation and high background signal. Arrows indicate MBGs powders.

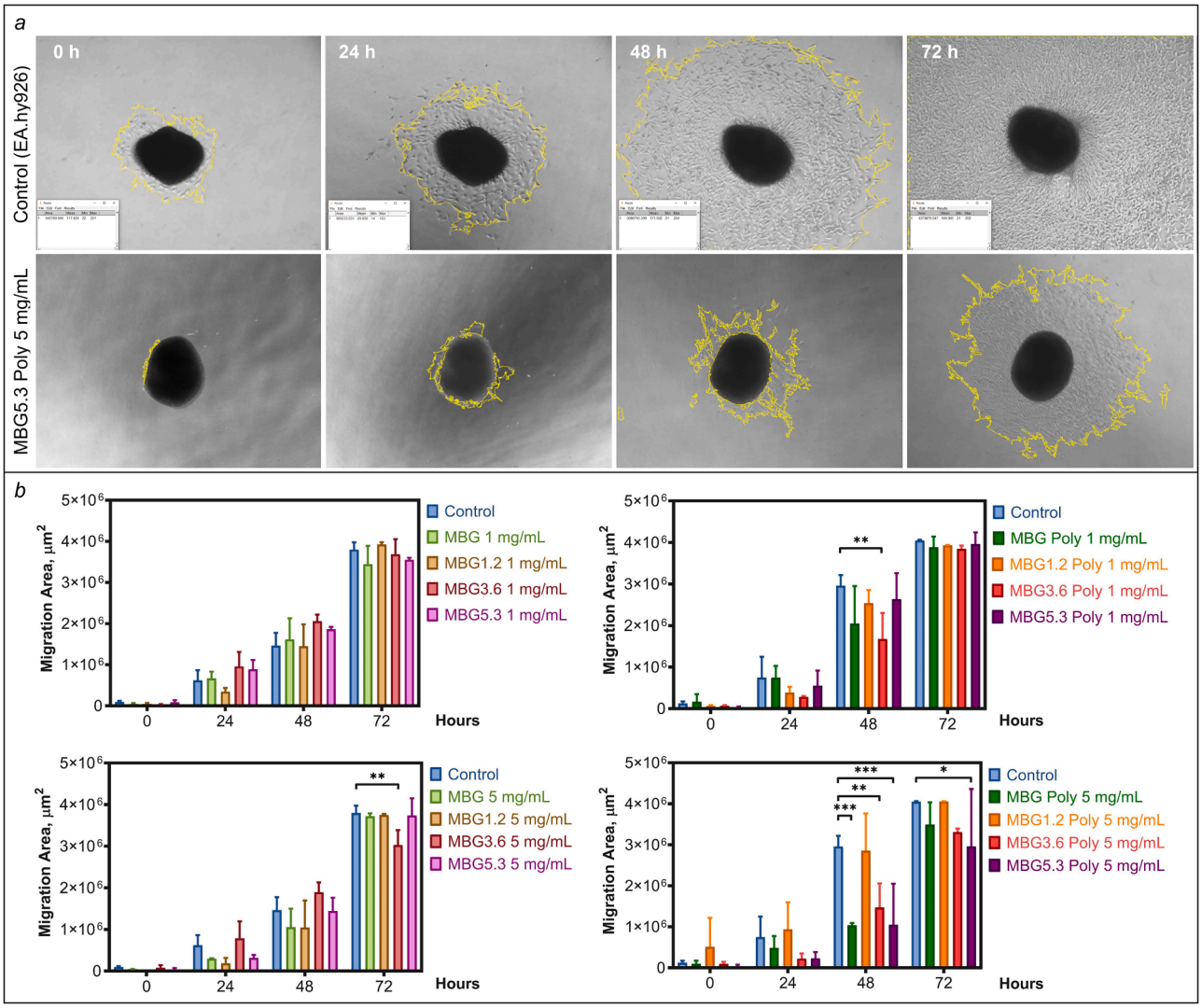

Fig. 3. Panel *a*: example of EA.hy926 spheroid migration quantitative analysis using ImageJ software (Control and MBG5.3 Poly 5 mg/mL groups). Panel *b*: EA.hy926 endothelial cell spheroids migration assay. Spheroids migration was analysed after 0, 24, 48, and 72 hrs of incubation with MBGs extracts. The values are presented as the mean of three biological replicates ± SD, * - significant difference compared to control, $p < 0.05$; ** - $p < 0.01$; *** - $p < 0.001$.

Model *in vitro*	2D hMSCs		3D hMSCs		2D U2OS		3D U2OS		3D EA.hy926	
MBG				*			**	**		
MBG1.2	*					**				
MBG3.6					*	*				**
MBG5.3				*	*	**				
MBG Poly			*	**						**
MBG1.2 Poly				**	*					
MBG3.6 Poly			*	**					**	**
MBG5.3 Poly			**							***
Concentration (mg/mL)	**1**	**5**	**1**	**5**	**1**	**5**	**1**	**5**	**1**	**5**

Fig. 4. Summary of MBGs *in vitro* testing. Red fields indicate either a decrease in metabolic activity (hMSCs and U2OS) or a decrease in cell migration rate (EA.hy926) compared to control. Asterisks indicate the level of significance: * - $p < 0.05$; ** - $p < 0.01$; *** - $p < 0.001$.

metabolic activity. In comparison to Ce-MBGs, MBG without cerium demonstrated the lowest relative cell viability (Fig. 5 (c), left), and in the case of Poly-functionalized pellets (Fig. 5 (c), right), U2OS cell metabolic activity has decreased comparably equally in all groups.

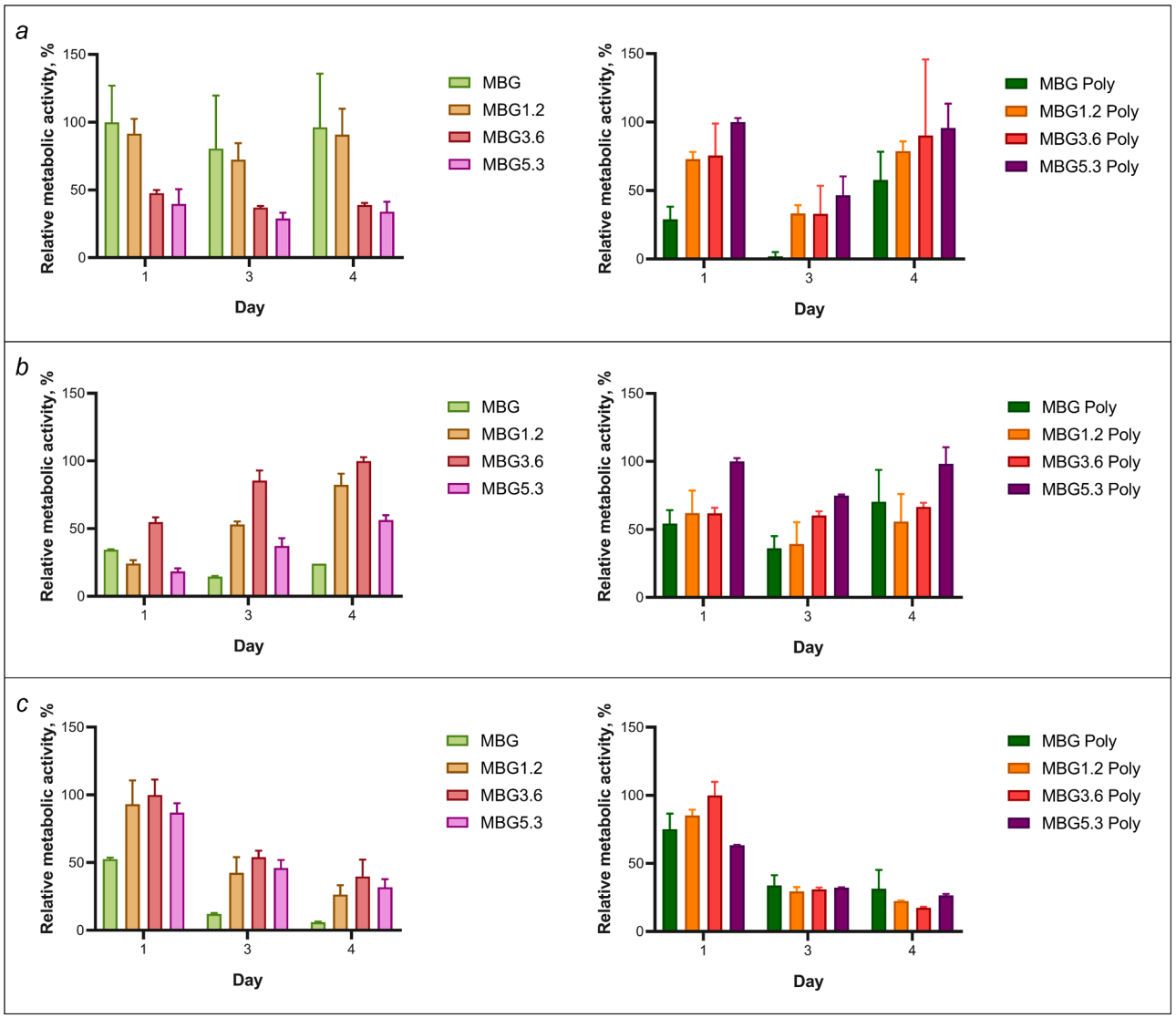

Fig. 5. Ce-MBGs and Ce-MBGs-Poly pellets compatibility towards hMSCs (a), EA.hy926 (b) and U2OS (c). Metabolic activity is presented as normalized means of relative fluorescent units of three biological replicates, and error bars represent SD.

4. Discussion

In this study, we performed the *in vitro* cytocompatibility evaluation of Ce-MBGs and Ce-MBGs-Poly, two types of bioactive glasses with distinct antioxidant properties. The intended use of these materials is their direct application to the site of a bone defect, including defects caused by bone tumor resection. Accordingly, we selected cell lines linked to bone repair and bone tumor growth: hMSCs, which are known to be recruited in the process of bone healing *in vivo*; osteosarcoma U2OS cells, which represent the possible tumor residues on the site of resection; and endothelial EA.hy926 cells as representatives of angiogenesis crucial for bone regeneration.

Modern approaches to the biological evaluation of materials encompass a wide variety of study designs aiming at approximating physiologically relevant conditions. Thus, standard monolayer-based approaches are being complemented with 3D-based ones [43,44]. However, it is debated whether 3D-based *in vitro* testing is more relevant than 2D *in vitro* testing for every type of cell and type of tested material. In this work, we considered both, and firstly evaluated the influence of direct contact with MBGs powders on the cells in a monolayer (2D), and then – in a spheroid-based (3D) model. Finally, considering the possible application of the material, we formed the pellets from the MBGs powders and tested their cytocompatibility by seeding the cells on their surface.

The heterogeneity of the results, which depends not only on the type of cells and presence of cerium and Poly but also on the testing approach (2D *vs* 3D), is of particular interest. For instance, the Ce-MBGs 1.2 (5 mg/mL), 3.6, and 5.3 (1 and 5 mg/mL) decrease the metabolic activity of U2OS in the monolayer-based model but do not demonstrate any cytotoxic effect towards U2OS spheroids; conversely, Ce-MBGs Poly 1.2 (5 mg/mL) and 3.6 (1 and 5 mg/mL) are not cytotoxic in the 2D model but inhibit proliferation of hMSCs spheroids.

One of the factors causing such diversity of results is the abundance of direct cell-material contact in 2D models: while in a cell monolayer, the cells are equally exposed to the powders, in a spheroid, only the cells present in the outer layer are exposed. Next, direct contact with the material surface may alter the fate of a cell: the bioactive ions and biomolecules (which are, in our case, cerium and Poly) are being released in the culture medium, altering thus the biochemical environment. Again, in contrast to cells in monolayer, there would be a gradient of cerium ions and Poly concentration reaching cells located in different layers of the spheroid [45]. We saw, however, that both U2OS and hMSCs spheroids tend to disaggregate with time (Fig. 2), so both these factors – dissimilar cell-material contact and exposure to the released

ions and biomolecules – might be an accurate explanation for the early incubation time points only.

Yet another factor to consider in the context of 2D *in vitro* models – especially, in the case of testing material in high concentrations – is the barrier created by the material between cells seeded on polystyrene and culture media. As could be observed in bright-field microscopy (Fig. S10), in comparison to 1 mg/mL concentration, MBGs at a concentration of 5 mg/mL were covering an overwhelming area of the cultured monolayer, possibly creating conditions in which cells experience nutrients and gas exchange deficiency.

Taking these factors together, there are technical drawbacks coupled with both types of *in vitro* models used – monolayer-based and spheroid-based, – as well as with the dosage of the tested material. Thus, we demonstrate in our study that a combination of distinct approaches, different cell lines, and amounts of the tested material provides a wider and more comprehensive observation of the material's cytocompatibility and cytotoxicity.

When testing MBGs pellets, we observed a correlation of results with 2D assays. For instance, there was a gradual decrease in metabolic activity of U2OS cells seeded on the top of the pellets in all tested groups – and we observed the same effect when culturing U2OS monolayer with MBGs at 5 mg/mL. Such correlation is expected since the overwhelming number of cells are being cultured in direct contact with a high amount of material – the same circumstances that are being created in a 2D monolayer model.

In our study, we also observed contrasting patterns of cell metabolic activity depending on functionalisation with Poly, which points to an ambiguous effect of dual MBGs loading. Poly have a complex biological role, as they act both as reductive radical scavengers and pathway modulators [46] on healthy tissues. Furthermore, in some specific settings, Poly can act as pro-oxidants, supposedly by complexation of transition metals [47]. Similarly, along with other research groups, we demonstrated the antioxidant activity of Ce-MBGs, but cerium nanoparticles are known to produce ROS at the lower pH values characteristic of the cancer environment, which contributes to their toxicity towards tumor cells [48,49]. This effect could be offset by the presence of antioxidant Poly, as observed on the U2OS monolayer model on which Ce-MBGs show cytotoxicity and Ce-MBGs-Poly does not.

This picture suggests a complex interplay between cerium doping and Poly functionalization, as evidenced by the discrepant results of Ce-MBGs and Ce-MBGs-Poly in different assay settings, and the choice of the most promising material should then be driven by a balance of their effect in the various assays. In this context, considering the initial objective of developing the material for bone tissue engineering able to tackle the balance between pro-regenerative and anti-tumorigenic activity, our attention is drawn mainly to the MBG1.2 Poly group in the lowest (1 mg/mL) concentration. This group was able to significantly inhibit the metabolic activity of U2OS cells maintaining at the same time the viability of hMSCs. Also, this material did not alter the migration ability of endothelial EA.hy926 cells.

Furthermore, our present findings correspond with observations of cerium release reported previously [16]. Ce-MBGs loaded with various biomolecules showed – regardless of the amount of cerium, – a cerium release about 1.6 % for MBGs loaded with gallic acid and anthocyanins, and about 3 % for MBGs loaded with polyphenols. MBG1.2 Poly were the most promising ones with the highest percentages. This trend is in agreement with the results of the more pronounced activity of MBG1.2 Poly against U2OS.

5. Conclusion

In our study, we examined the *in vitro* cytocompatibility of two types of mesoporous bioactive glasses with different antioxidant properties designed for bone tissue engineering, including tumor resection: MBGs doped with cerium and dually loaded with both cerium and polyphenols. By using both 2D and 3D *in vitro* models and relevant cell lines, we were able to demonstrate a complex relationship between the experimental design, material composition and dosage, and cellular responses. Variations in cytotoxicity between the 2D and 3D models highlighted how important it is to take different physiological circumstances into account. Factors such as direct cell-material contact, the release of bioactive ions, and potential nutrient barrier effects influenced outcomes of cell metabolic activity, cell morphology, cell membrane integrity, and migration assays. Furthermore, functionalization with polyphenols exhibited contrasting effects, showing mitigated cytotoxicity in comparison to Ce-MBGs without loading, suggesting a role in modulating oxidative stress responses. Supported by our previous observations of cerium release, the MBG1.2 Poly group at 1 mg/mL concentration emerged as promising, inhibiting osteosarcoma cell metabolic activity while preserving hMSCs viability and endothelial cell migration. These findings highlight the importance of comprehensive evaluation approaches integrating diverse assay settings and cell types to enhance bioactive glasses research, as well as the need for further investigations of the biological effects of dual doping of MBGs with agents with distinct mechanisms of antioxidant activity.

Funding

This work was supported by the European Union's H2020-MSCA-ITN [grant number 860462 (PREMUROSA)].

Declaration of generative AI and AI-assisted technologies in the writing process

During the preparation of this work, the authors used Grammarly in order to increase the quality of writing. After using this tool, the authors reviewed and edited the content as needed and take full responsibility for the content of the publication.

CRediT authorship contribution statement

Ksenia Menshikh: Writing – original draft, Visualization, Formal analysis, Investigation, Writing – review & editing. **Ajay Kumar Reddy:** Writing – original draft, Visualization, Formal analysis, Investigation, Writing – review & editing. **Andrea Cochis:** Conceptualization, Writing – original draft, Writing – review & editing. **Francesca Fraulini:** Writing – original draft, Visualization, Formal analysis, Investigation, Writing – review & editing. **Alfonso Zambon:** Conceptualization, Writing – original draft, Writing – review & editing. **Gigliola Lusvardi:** Conceptualization, Writing – review & editing, Funding acquisition. **Lia Rimondini:** Conceptualization, Writing – review & editing, Funding acquisition.

Declaration of competing interest

The authors do not have any conflicts of interest to declare.

Data availability

Data will be made available on request.

Supplementary materials

Supplementary material associated with this article can be found, in the online version, at doi:10.1016/j.bbiosy.2024.100095.

References

[1] Baino F, Hamzehlou S, Kargozar S. Bioactive glasses: where are we and where are we going? J Funct Biomater 2018;9:25. https://doi.org/10.3390/jfb9010025.
[2] Hench LL. The story of bioglass®. J Mater Sci Mater Med 2006;17:967–78. https://doi.org/10.1007/s10856-006-0432-z.

[3] El-Rashidy AA, Roether JA, Harhaus L, Kneser U, Boccaccini AR. Regenerating bone with bioactive glass scaffolds: a review of *in vivo* studies in bone defect models. Acta Biomater 2017;62:1–28. https://doi.org/10.1016/j.actbio.2017.08.030.

[4] Zheng K, Niu W, Lei B, Boccaccini AR. Immunomodulatory bioactive glasses for tissue regeneration. Acta Biomater 2021;133:168–86. https://doi.org/10.1016/j.actbio.2021.08.023.

[5] Rosenfeldt F, Wilson M, Lee G, Kure C, Ou R, Braun L, et al. Oxidative stress in surgery in an ageing population: pathophysiology and therapy. Exp Gerontol 2013;48:45–54. https://doi.org/10.1016/j.exger.2012.03.010.

[6] Firuzi O, Miri R, Tavakkoli M, Saso L. Antioxidant therapy: current status and future prospects. Curr Med Chem 2011;18:3871–88. https://doi.org/10.2174/092986711803414368.

[7] Kargozar S, Hooshmand S, Hosseini SA, Gorgani S, Kermani F, Baino F. Antioxidant effects of bioactive glasses (BGs) and their significance in tissue engineering strategies. Molecules 2022;27:6642. https://doi.org/10.3390/molecules27196642.

[8] Zhu H, Zheng K, Boccaccini AR. Multi-functional silica-based mesoporous materials for simultaneous delivery of biologically active ions and therapeutic biomolecules. Acta Biomater 2021;129:1–17. https://doi.org/10.1016/j.actbio.2021.05.007.

[9] O'Neill E, Awale G, Daneshmandi L, Umerah O, Lo KH. The roles of ions on bone regeneration. Drug Discov Today 2018;23:879–90. https://doi.org/10.1016/j.drudis.2018.01.049.

[10] Mouriño V, Vidotto R, Cattalini JP, Boccaccini AR. Enhancing biological activity of bioactive glass scaffolds by inorganic ion delivery for bone tissue engineering. Curr Opin Biomed Eng 2019;10:23–34. https://doi.org/10.1016/j.cobme.2019.02.002.

[11] Wason MS, Zhao J. Cerium oxide nanoparticles: potential applications for cancer and other diseases. Am J Transl Res 2013;5:126–31.

[12] Zambon A, Malavasi G, Pallini A, Fraulini F, Lusvardi G. Cerium containing bioactive glasses: a review. ACS Biomater Sci Eng 2021;7:4388–401. https://doi.org/10.1021/acsbiomaterials.1c00414.

[13] Nicolini V, Gambuzzi E, Malavasi G, Menabue L, Menziani MC, Lusvardi G, et al. Evidence of catalase mimetic activity in Ce^{3+}/Ce^{4+} doped bioactive glasses. J Phys Chem B 2015;119:4009–19. https://doi.org/10.1021/jp511737b.

[14] Leonelli C, Lusvardi G, Malavasi G, Menabue L, Tonelli M. Synthesis and characterization of cerium-doped glasses and *in vitro* evaluation of bioactivity. J Non Cryst Solids 2003;316:198–216. https://doi.org/10.1016/S0022-3093(02)01628-9.

[15] Nicolini V, Malavasi G, Lusvardi G, Zambon A, Benedetti F, Cerrato G, et al. Mesoporous bioactive glasses doped with cerium: Investigation over enzymatic-like mimetic activities and bioactivity. Ceram Int 2019;45:20910–20. https://doi.org/10.1016/j.ceramint.2019.07.080.

[16] Lusvardi G, Fraulini F, D'Addato S, Zambon A. Loading with biomolecules modulates the antioxidant activity of cerium-doped bioactive glasses. ACS Biomater Sci Eng 2022;8:2890–8. https://doi.org/10.1021/acsbiomaterials.2c00283.

[17] Łapa A, Cresswell M, Campbell I, Jackson P, Goldmann WH, Detsch R, et al. Ga and Ce ion-doped phosphate glass fibres with antibacterial properties and their composite for wound healing applications. J Mater Chem B 2019;7:6981–93. https://doi.org/10.1039/C9TB00820A.

[18] Atkinson I, Seciu-Grama AM, Petrescu S, Culita D, Mocioiu OC, Voicescu M, et al. Cerium-containing mesoporous bioactive glasses (MBGs)-derived scaffolds with drug delivery capability for potential tissue engineering applications. Pharmaceutics 2022;14:1169. https://doi.org/10.3390/pharmaceutics14061169.

[19] Zheng K, Torre E, Bari A, Taccardi N, Cassinelli C, Morra M, et al. Antioxidant mesoporous Ce-doped bioactive glass nanoparticles with anti-inflammatory and pro-osteogenic activities. Mater Today Bio 2020;5:100041. https://doi.org/10.1016/j.mtbio.2020.100041.

[20] Cazzola M, Vernè E, Cochis A, Sorrentino R, Azzimonti B, Prenesti E, et al. Bioactive glasses functionalized with polyphenols: *in vitro* interactions with healthy and cancerous osteoblast cells. J Mater Sci 2017;52:9211–23. https://doi.org/10.1007/s10853-017-0872-5.

[21] Ferraris S, Miola M, Cochis A, Azzimonti B, Rimondini L, Prenesti E, et al. *In situ* reduction of antibacterial silver ions to metallic silver nanoparticles on bioactive glasses functionalized with polyphenols. Appl Surf Sci 2017;396:461–70. https://doi.org/10.1016/j.apsusc.2016.10.177.

[22] Sayed Abdelgeliel A, Ferraris S, Cochis A, Vitalini S, Iriti M, Mohammed H, et al. Surface functionalization of bioactive glasses with polyphenols from padina pavonica algae and *in situ* reduction of silver ions: physico-chemical characterization and biological response. Coatings 2019;9:394. https://doi.org/10.3390/coatings9060394.

[23] Schuhladen K, Roether JA, Boccaccini AR. Bioactive glasses meet phytotherapeutics: the potential of natural herbal medicines to extend the functionality of bioactive glasses. Biomaterials 2019;217:119288. https://doi.org/10.1016/j.biomaterials.2019.119288.

[24] Torre E, Iviglia G, Cassinelli C, Morra M, Russo N. Polyphenols from grape pomace induce osteogenic differentiation in mesenchymal stem cells. Int J Mol Med 2020. https://doi.org/10.3892/ijmm.2020.4556.

[25] Cazzola M, Ferraris S, Boschetto F, Rondinella A, Marin E, Zhu W, et al. Green tea polyphenols coupled with a bioactive titanium alloy surface: *in vitro* characterization of osteoinductive behavior through a KUSA A1 cell study. Int J Mol Sci 2018;19:2255. https://doi.org/10.3390/ijms19082255.

[26] Zhang X, Ferraris S, Prenesti E, Verné E. Surface functionalization of bioactive glasses with natural molecules of biological significance, Part I: gallic acid as model molecule. Appl Surf Sci 2013;287:329–40. https://doi.org/10.1016/j.apsusc.2013.09.151.

[27] Zhang X, Ferraris S, Prenesti E, Verné E. Surface functionalization of bioactive glasses with natural molecules of biological significance, part II: grafting of polyphenols extracted from grape skin. Appl Surf Sci 2013;287:341–8. https://doi.org/10.1016/j.apsusc.2013.09.152.

[28] Corazzari I, Tomatis M, Turci F, Ferraris S, Bertone E, Prenesti E, et al. Gallic acid grafting modulates the oxidative potential of ferrimagnetic bioactive glass-ceramic SC-45. Colloids Surf B Biointerfaces 2016;148:592–9. https://doi.org/10.1016/j.colsurfb.2016.09.034.

[29] Riccucci G, Cazzola M, Ferraris S, Gobbo VA, Miola M, Bosso A, et al. Surface functionalization of bioactive glasses and hydroxyapatite with polyphenols from organic red grape pomace. J Am Ceram Soc 2022;105:1697–710. https://doi.org/10.1111/jace.17849.

[30] Torre E, Iviglia G, Cassinelli C, Morra M. Potentials of polyphenols in bone-implant devices. Polyphenols. InTech; 2018. https://doi.org/10.5772/intechopen.76319.

[31] Baino F, Novajra G, Miguez-Pacheco V, Boccaccini AR, Vitale-Brovarone C. Bioactive glasses: special applications outside the skeletal system. J Non Cryst Solids 2016;432:15–30. https://doi.org/10.1016/j.jnoncrysol.2015.02.015.

[32] Diomede F, Marconi GD, Fonticoli L, Pizzicanella J, Merciaro I, Bramanti P, et al. Functional relationship between osteogenesis and angiogenesis in tissue regeneration. Int J Mol Sci 2020;21:3242. https://doi.org/10.3390/ijms21093242.

[33] Xie H, Sha S, Lu L, Wu G, Jiang H, Boccaccini AR, et al. Cerium-containing bioactive glasses promote *in vitro* lymphangiogenesis. Pharmaceutics 2022;14. https://doi.org/10.3390/pharmaceutics14020225.

[34] Jablonská E, Horkavcová D, Rohanová D, Brauer DS. A review of: *In vitro* cell culture testing methods for bioactive glasses and other biomaterials for hard tissue regeneration. J Mater Chem B 2020;8:10941–53. https://doi.org/10.1039/d0tb01493a.

[35] Brookes MJ, Chan CD, Baljer B, Wimalagunaratna S, Crowley TP, Ragbir M, et al. Surgical advances in osteosarcoma. Cancers 2021;13:1–26. https://doi.org/10.3390/cancers13030388.

[36] Wittmaack K. Excessive delivery of nanostructured matter to submersed cells caused by rapid gravitational settling. ACS Nano 2011;5:3766–78. https://doi.org/10.1021/nn200112u.

[37] Klimek K, Belcarz A, Pazik R, Sobierajska P, Han T, Wiglusz RJ, et al. "False" cytotoxicity of ions-adsorbing hydroxyapatite — corrected method of cytotoxicity evaluation for ceramics of high specific surface area. Mater Sci Eng C 2016;65:70–9. https://doi.org/10.1016/j.msec.2016.03.105.

[38] Fröhlich E. Comparison of conventional and advanced *in vitro* models in the toxicity testing of nanoparticles. Artif Cells Nanomed Biotechnol 2018;46:1091–107. https://doi.org/10.1080/21691401.2018.1479709.

[39] Varini E, Sánchez-Salcedo S, Malavasi G, Lusvardi G, Vallet-Regí M, Salinas AJ. Cerium (III) and (IV) containing mesoporous glasses/alginate beads for bone regeneration: bioactivity, biocompatibility and reactive oxygen species activity. Mater Sci Eng C 2019;105:109971. https://doi.org/10.1016/j.msec.2019.109971.

[40] James S, Fox J, Afsari F, Lee J, Clough S, Knight C, et al. Multiparameter analysis of human bone marrow stromal cells identifies distinct immunomodulatory and differentiation-competent subtypes. Stem Cell Rep 2015;4:1004–15. https://doi.org/10.1016/j.stemcr.2015.05.005.

[41] Bäcker V. Analyze Spheroid cell invasion In 3D matrix, RRID:SCR_021204 2012. https://github.com/MontpellierRessourcesImagerie/imagej_macros_and_scripts/wiki/Analyze-Spheroid-Cell-Invasion-In-3D-Matrix (accessed February 13, 2024).

[42] Fraulini F, Raimondi S, Candeliere F, Ranieri R, Zambon A, Lusvardi G. Ce-MBGs loaded with gentamicin: characterization and *in vitro* evaluation. J Funct Biomater 2023;14:129. https://doi.org/10.3390/jfb14030129.

[43] De Jong WH, Carraway JW, Geertsma RE. *In vivo* and *in vitro* testing for the biological safety evaluation of biomaterials and medical devices. Biocompatibility and performance of medical devices. Elsevier; 2019. p. 123–66. https://doi.org/10.1016/B978-0-08-102643-4.00007-0.

[44] Frisch E, Clavier L, Belhamdi A, Vrana NE, Lavalle P, Frisch B, et al. Preclinical *in vitro* evaluation of implantable materials: conventional approaches, new models and future directions. Front Bioeng Biotechnol 2023;11. https://doi.org/10.3389/fbioe.2023.1193204.

[45] Białkowska K, Komorowski P, Bryszewska M, Miłowska K. Spheroids as a type of three-dimensional cell cultures—examples of methods of preparation and the most important application. Int J Mol Sci 2020;21:6225. https://doi.org/10.3390/ijms21176225.

[46] Cháirez-Ramírez MH, de la Cruz-López KG, García-Carrancá A. Polyphenols as antitumor agents targeting key players in cancer-driving signaling pathways. Front Pharmacol 2021;12. https://doi.org/10.3389/fphar.2021.710304.

[47] Symonowicz M, Kolanek M. Flavonoids and their properties to form chelate complexes. Biotechnol Food Sci 2012;76:35–41. https://doi.org/10.34658/bfs.2012.76.1.35-41.

[48] Lord MS, Berret JF, Singh S, Vinu A, Karakoti AS. Redox active cerium oxide nanoparticles: current status and burning issues. Small 2021;17. https://doi.org/10.1002/smll.202102342.

[49] Cheng H, Lin S, Muhammad F, Lin YW, Wei H. Rationally modulate the oxidase-like activity of nanoceria for self-regulated bioassays. ACS Sens 2016;1:1336–43. https://doi.org/10.1021/acssensors.6b00500.